Egyptian Journal of Basic and Clinical Pharmacology
December 2017, Vol. 7, No. 2: 9-24
http://www.ejbcp.eg.net/

Original Article

Evaluation of the Therapeutic Effects of Polyvinylpyrrolidone-Capped Silver Nanoparticles on the Diethylnitrosamine/Carbon Tetrachloride-Induced Hepatocellular Carcinoma in Rats

Samah M. Elaidy[1*], Amr Moghazy[2], and Mohamed K. El-Kherbetawy[3]
[1]*Department of Clinical Pharmacology, Faculty of Medicine, Suez Canal University, Egypt*
[2]*Department of Plastic Surgery, Faculty of Medicine, Suez Canal University, Egypt.*
[3]*Department of Pathology, Faculty of Medicine, Suez Canal University, Egypt.*

A B S T R A C T

Globally, hepatocellular carcinoma (HCC) is the second-ranked cause of cancer-related deaths. Induction of anti-angiogenesis and apoptosis are highly effective strategies for treating HCC. Emergence of the anti-angiogenic and apoptotic properties of silver nanoparticles (AgNP) is a developing policy in cancer therapy. The present study was conducted to evaluate the therapeutic effects of polyvinylpyrrolidone (PVP)-capped AgNPs on chemically-induced HCC in rats. Induction of HCC model in male albino Wistar rats (220-250 g) was initiated by a single intraperitoneal injection of diethylnitrosamine (DEN; 200 mg/kg), then after 2 weeks promoted intraperitoneally with carbon tetrachloride (CCl_4) solution (CCl_4/olive oil; 1:1; 1 ml/kg) three times weekly for 6 weeks. HCC was confirmed through significant reductions in survival rates, serum albumin, elevations in serum alanine aminotransferase (ALT), aspartate aminotransferase (AST) and alpha-fetoprotein (AFP) levels and hepatic vascular endothelial growth factors (VEGF), platelet-derived growth factors (PDGF), nitric oxide (NO), interleukin (Il)-4 and -8, and tumor necrosis factor-alpha (TNF-α) levels, in addition to the histopathological dysplastic changes. PVP-AgNPs (30, 125, and 300 mg/kg/day) were given through oral gavage for 28 days. PVP-AgNPs therapy showed significant amelioration of these injurious effects with enhancement in the hepatic caspases activities, translated histopathologically to a marked improvement in the hepatic architecture. PVP-AgNPs 125mg/kg/day regimens displayed the best therapeutic effects, which considered a therapeutic modality for HCC regarding their anti-inflammatory, antiangiogenic, and caspase-dependent apoptotic effects. Advanced targeted molecular studies for use of single or combined regimens of PVP-AgNPs with different chemotherapeutics are recommended.

Key Words: Alpha-fetoprotein, Angiogenesis, Apoptosis, Carbon tetrachloride, Diethylinitrosamine, Hepatocellular Carcinoma, Polyvinylpyrrolidone-capped silver nanoparticles.

Corresponding Author: *Samah M. Elaidy* **Email:** *semsemologist@yahoo.com*
samah_elaidi@med.suez.edu.eg

1. INTRODUCTION

Hepatocellular carcinoma (HCC), the fifth most common malignancy, is the second-most common cause of cancer-related deaths worldwide, due to its poor general prognosis **(Njei et al., 2015; Yu, 2016)**.

The HCC is an extremely vascularized tumor, in which angiogenesis has a critical role in the progression, metastasis, and recurrence **(Yang et al., 2014; Muto et al., 2015)**. One of the angiogenic stimulating factors is oxidative stress/inflammatory cascade. It enhances the vascular permeability and chemokine-mediated enrolment of leukocytes and platelets with major angiogenic cytokines and growth factors release. The most important of these are nitric oxide (NO), vascular endothelial growth factor (VEGF), platelet-derived growth factor (PDGF), interleukin-4 (IL-4), IL-8, and tumor necrosis factor-alpha (TNF-α) **(Sanz-Cameno et al., 2010; Muto et al., 2015)**.

Furthermore, dysregulated apoptosis has a crucial role in HCC tumorigenesis and acquired resistance to chemotherapy. Caspase-3 cleavage is a mutual step in the intrinsic (mitochondrial), and extrinsic apoptotic cellular pathways, with dependent roles of caspase-9 and TNF-α/caspase-8, respectively **(Fabregat, 2009; Wong, 2011; Yin et al., 2015)**.

The hepatic-drug targeting, as well as handling of the different apoptotic and anti-angiogenic cascades resulting in evidenced anti-proliferative effects, are

possessing remarkable HCC therapeutic promises **(Bishayee and Darvesh, 2012; Yang et al., 2014; Muto et al., 2015)**. Moreover, with Food and Drug Administration (FDA) limited approval for HCC valuable effective therapeutic options due to marked adverse effects and the emergence of resistance, new drug regimens are in crucial need, as a seldom entity or as an adjuvant for enhancement and resistance reduction **(Fornari et al., 2017)**.

Silver nanoparticles (AgNPs), are the best-recognized nanoproducts that have been applied widely especially as antimicrobial agents **(Hussein and Sarhan, 2014)**. The AgNps are displaying selective hepatic deposition with enhanced hepatic first-pass effects after in-vivo oral administration **(Kim et al., 2010; Jiménez-Lamana et al., 2014)**, with remarkable engulfment by the malignant cells, away from the surrounding normal cells, and a lacking recovery from their effects **(AshaRani et al., 2009; Perrault et al., 2009; Prabhu et al., 2011)**.

The AgNP prevents VEGF-stimulated angiogenesis as well as cellular proliferation and migration induced by activated phosphatidylinositol-3-kinases/Protein kinase B (PI3K/Akt) signaling pathways **(Gurunathan et al., 2009; Kalishwaralal et al., 2009)**. Moreover, different cytotoxic effects and reduction in cellular viabilities ending in anti-proliferative effects through oxidative stress-apoptotic pathways were recognized by using AgNP both in various cancer cell lines including human hepatocellular carcinoma HePG-2 cell line **(Zhu et al., 2016)**, and other *in vivo* cancer models regardless HCC models **(Hsin et al., 2008; çIftçI et al., 2013; Sun et al., 2013)**.

These special characters of AgNP fulfill the criteria of the effective HCC anticancer agents regarding the hepatic targeting, anti-angiogenic properties, and apoptotic cytotoxicity, with low cost synthesis. Thus, the current study rationale was about the possible therapeutic roles of AgNP in different doses on *in vivo* HCC animal model.

2. MATERIALS AND METHODS

2.1. Drugs and chemicals

- Diethylnitrosamine (N-nitrosodiethylamine; DEN; purity, 99.0%), carbon tetrachloride (CCl_4), and nitric oxide (NO) colorimetric assay kits were purchased from Sigma-Aldrich Company, St. Louis., USA.
- The PVP-AgNp was provided by Nanotech Company, Egypt.
- The enzyme-linked immunosorbent assay (ELISA) kits for IL-4, VEGF, PDGF-BB, and TNF-α were obtained from Quantikine® ELISA, R&D systems, Minneapolis, MN, USA, while those for alpha-fetoprotein (AFP), and IL-8 was purchased from MyBioSource Company, San Diego, USA.
- Caspase-3, -8 and -9 colorimetric assay kits were purchased from Abcam Company; Cambridge, U.K.
- All other chemicals and drugs were purchased from Sigma-Aldrich Company, St. Louis., USA.

2.2. Animals

Male albino Wistar rats (220 - 250 g) were brought from the Egyptian Organization for Biological Products and Vaccines, Cairo, Egypt. Rats were allowed free access to food and water and were maintained under standard conditions (normal light/dark cycle, and temperature 25 ± 3 °C). Animals were left to acclimatize for one week before starting the experiment. All experimental dealings were approved by the Institutional Animal Care and Use Committee of the Suez Canal University, which is following the National Institutes of Health guide for the care and use of laboratory animals (Maryland, USA) as a benchmark.

2.3. Experimental protocol

2.3.1. Polyvinylpyrrolidone-capped silver nanoparticles preparation and characterization

Polyvinylpyrrolidone (PVP) capped-AgNP was supplied as a transparent grayish yellow-water-soluble liquid (5 ml, 512mg/ml phosphate buffer saline, 99.98% purity), after chemical reduction preparation method as reported by **(Lee and Meisel, 1982)** and **(Pacioni et al., 2015)**. Briefly, a solution of $AgNO_3$ was used as Ag1+ ions precursor, while sodium borohydride ($NaBH_4$) and PVP was used as mild reducing, and stabilizing agents, respectively. The color of the solution slowly turned into grayish-yellow; indicating the reduction of the Ag1+ ions to Ag nanoparticles.

The PVP-AgNP was in a uniform spherical-shaped particles with particle size around 20 nm, which was characterized using transmission electron microscopy (TEM; JEOL JEM-2100 high-resolution TEM at an accelerating voltage of 200 kV), as shown in **Figure (1A)**. The ultraviolet visual (UV-Vis) absorption spectrum (λ_{max}) was at 403 nm; **Figure (1B)**, was obtained on an Ocean Optics USB2000+VIS-NIR Fiber optics spectrophotometer. Before each use, the solution was sonicated for 10 min to ensure uniform distribution of the nanoparticles.

2.3.2. Chemical induction of HCC

Induction of HCC was through two consecutive stages: initiation and promotion by DEN and CCl_4; respectively **(Zalatnai and Lapis, 1994; Abdel aziz et al., 2011; Motawi et al., 2016)**. For initiation, DEN was administered in a single intraperitoneal (IP) dose of 200 mg/kg dissolved in normal saline 0.9% at a final volume of 1ml/kg. Two weeks after DEN challenging, CCl_4 solution (CCl_4/olive oil; 1:1; 1 ml/kg) was administered IP three times weekly for 6 consecutive weeks.

2.3.3. Study groups

The PVP-AgNPs were used in three different doses: a dose of 30 mg/kg/day representing the No Observed Adverse Effect Level (NOAEL), a dose of 125

mg/kg/day, and a dose of 300 mg/kg/day which was considered the Lowest Observable Adverse Effect Level (LOAEL) for 28 days in two different rat species according to safety profiles mentioned by **(Kim et al., 2010; Jiménez-Lamana et al., 2014)**. Experimental rats were randomly divided into 8 groups of 12 animals each. **Normal-untreated group;** where normal rats were not given any medications, **PVP-AgNPs (30)-, (125)- and (300)-control groups**; where PVP-AgNPs were given by oral gavage in a dose of 30, 125 and 300 mg/kg/day for 28 days, respectively **(Kim et al., 2010)**, and finally **DEN/CCl_4-control group** where included rats who developed HCC were not given any treatment. By the start of the 9th week after DEN injection, rats were subjected for 28 days to daily oral gavage of normal saline. **PVP-AgNPs (30)-, (125)- and (300)-treated group**s; After induction of HCC, PVP-AgNPs were daily given by oral gavage in doses of 30, 125 and 300 mg/kg body weight from the start of the 9th week for 28 days.

2.4. Blood and hepatic sampling and processing

Twenty-four hours after the last injections, blood samples for biochemical and biological analyses were collected from individual anesthetized rats through retro-orbital plexus, then cervical decapitation was done. The collected blood was left to coagulate. After centrifugation at 4000 r.p.m. for 10 min (4°C), sera were separated and used for determination of aspartate aminotransferase (AST), alanine aminotransferase (ALT), and AFP levels. Each liver was dissected out, washed in cold normal saline, and dissected into two parts. One part was embedded in 10% neutral buffered formalin for the histopathological examinations, while the other was rapidly frozen in liquid nitrogen and kept in -80ºC for the further measurement of hepatic NO, Il-4, -8, VEGF, PDGF-BB, and TNF-α levels and caspase-3, -8 and -9 assays.

2.5. Assays for serum liver enzymes, and AFP levels

Serum liver enzymes were measured spectrophotometrically with the Hitachi 912 (Roche Diagnostics Co., Mannheim, Germany) as previously instructed **(Huo et al., 2011)**. AFP, a commonly used tumor marker for HCC assays was measured according to the manufacturer instructions **(Billmire et al., 2014)**.

2.6. Total hepatic No, VEGF, PDGF-BB, IL-4, IL-8, and TNF-α assays

Each liver tissue was weighed, homogenized in phosphate buffer saline (PBS), centrifuged at 14000×g for 10 min (4°C) and the supernatant was used for further analyses. Liver content of NO was measured according to the previous method described by **Montgomery et al. (1962)** using the manufacturer kits. For quantification of VEGF, PDGF-BB, IL-4, IL-8, and TNF-α contents, each liver homogenate was assessed as instructed in the commercial ELISA kits using an ELISA reader (Metertech, M960) **(Chen et al., 2008)**.

2.7. Colorimetric assay of the protease activity of caspase-3, -8 and -9

Caspases apoptotic activities measurement was performed using colorimetric kits in accordance with the manufacturer's instructions (Abcam Company; Cambridge, U.K).

2.8. Histopathological examinations

Liver tissues, preserved in neutral buffered formalin 10% solution, were processed to obtain Formalin Fixed Paraffin Embedded (FFBE) blocks. Changes were assessed in histopathological sections at 3-micron cuts stained with hematoxylin and eosin (H&E) stains. A histopathological modified score of HCC was applied according to a histopathological score. This score evaluated the hepatic architecture as 0 for preserved architecture and 1 for disturbed architecture. The nuclear to cytoplasmic (N/C) ratio was assessed as (0) for normal ratio (1:4), (1) for mild increased ratio (1:3), (2) for moderate increased ratio (1:2), and (3) for markedly increased ratio (≥1:1). The degree of pleomorphism was assessed as grade (0) for no findings to minimal nuclear irregularity, grade (1) for hyperchromatism, prominent nucleoli, and some irregular nuclei, grade (2) for changes more than grade (1) besides angulated nuclei, and grade (3) for noticeable pleomorphism with anaplastic giant cells (Paradis, 2013). Finally, the degenerative hydropic changes or steatosis was scored as (0) for < 5%, (1) for 5%-33%, (2) for > 33%-66%, and (3) for > 66% (Kleiner et al., 2005).

2.9. Statistical analysis

Results were collected and expressed as a mean ± standard error of the mean (SEM) then analyzed using the statistical package for the social sciences (SPSS Software, SPSS Inc., Chicago, USA), version 23. One-way analysis of variance (ANOVA) followed by post-hoc multiple comparisons; Bonferroni test was used to test the significance of the difference between quantitative variables. Other categorical values were assessed by using Chi-square test with Yates's correction. Survival data were assessed by the Kaplan–Meier analysis using Log-Rank test. A p-value < 0.05 was considered to be statistically significant.

3. RESULTS

3.1. Effects of PVP-AgNPs on the survival percentages

As shown in **Figure (2)**, the survival rates were plotted. The survival rates of the AgNPs control groups revealed insignificant changes in comparison to the control-untreated group (not shown; $p > 0.05$). In DEN/CCl_4-control group, a low survival percentage (58%) were found, which was significantly lower than the normal control group's survival percentage (100%; $p < 0.05$). After DEN/CCl_4-challenging, treatments with AgNPs (30), (125), and (300) showed higher significant

survival percentages, 67%, 92%, and 83%; respectively, with significant differences between the therapeutic modalities ($p > 0.05$).

3.2. Effects on serum liver enzymes, albumin, and AFP levels

As shown in **Table (1)**, in normal healthy rats, the oral daily administration of PVP-AgNPs in doses of 30 and 125 mg/kg didn't induce significant changes in means serum liver enzymes, albumin, and AFP levels when compared to the normal-untreated group ($p > 0.05$). While, the PVP-AgNPs in a dose of 300 mg/kg/day showed a significant elevation in means serum liver enzymes, and a significant reduction in means serum albumin levels in comparison to the normal untreated group ($p < 0.05$), without significant alterations in the AFP levels ($p > 0.05$). The DEN/CCl4-challenging displayed significantly higher levels of means serum liver enzymes, and AFP, and lower levels of mean serum albumin ($p < 0.05$), which ameliorated by the administration of PVP-AgNPs in different doses. The PVP-AgNPs in a dose of 125mg/kg/day showed the most ameliorated levels in comparison to PVP-AgNPs (30)-, and (300)-treated groups ($p < 0.05$).

3.3. Effects on hepatic NO, VEGF, PDGF-B, Il-4, Il-8, and TNF-α levels

The PVP-AgNPs administration in different doses did not alter the mean hepatic levels of the pro/angiogenic mediators including NO, VEGF, and PDGF-B, beside Il-4, Il-8, and TNF-α in comparison to the normal-untreated group ($p > 0.05$). The challenging with DEN/CCl_4 displayed significant elevations in means hepatic levels of VEGF, PDGF-B, and Il-4, Il-8, and TNF-α compared to the normal-untreated rats ($p < 0.05$). Different regimens of PVP-AgNPs significantly ameliorated these deleterious changes-induced by DEN/CCl_4 ($p < 0.05$), to be comparable to the normal-untreated group ($p > 0.05$). Furtherly, the PVP-AgNPs in a dose of 125 mg/kg/day revealed the most significant improvements compared to the other treated groups ($p < 0.05$), **Figure (3A)** and **(B)**.

3.4. Changes in total hepatic caspase-3, -8 and -9 activities

In normal healthy rats, after administration of the PVP-AgNPs (125), and (300), the hepatic activities of caspase-3, -8 and -9 were augmented significantly in comparison to the normal-untreated group ($p < 0.05$). Administration of DEN/CCl_4 showed insignificant increases in the hepatic caspases activities ($p > 0.05$). Therapeutic regimens with different doses of PVP-AgNPs showed amplifications in these proteolytic activities ($p < 0.05$), which were most evident after the PVP-AgNPs (300) administration ($p < 0.05$), **Figure (4)**.

3.5. Effects on DEN/CCl_4-induced hepatic histopathological changes

As shown in **Figure (5) and Table (2),** the normal-untreated, the PVP-AgNP (30), (125)-, and (300)-control groups showed normal hepatocytes arranged in plates of one/two cell thickness, surrounding patent sinusoids with abundant eosinophilic cytoplasm, central vesicular nucleus with inconspicuous nucleoli (N/C ratio of 1:4). After DEN/CCl_4 challenging, high histopathological scores with disturbed architecture with thick plates, nests, and sheets of hepatocytes were evidenced. The hepatocytes exhibited markedly enlarged nuclei, markedly increased N/C ratio of 1:1 or more, and coarse chromatin-containing nuclei. Some hepatocytes showing more than one prominent nucleolus, and scattered binucleated and multinucleated cells. There was moderate pleomorphism with few apoptotic and necrotic cells. The PVP-AgNP (30)-treated groups showed mild improvement in the architecture, while the PVP-AgNP (300)-treated group showed moderate restored architecture. The PVP-AgNPs (125)-treated group showed marked restoration of lobular architecture and normal characteristics of the hepatocytes, **Figure (5) and Table (2)**.

Table (1): Changes in means serum liver enzymes activities, albumin, and AFP levels in different study groups.

Study Groups (n=12)	Serum ALT (U/L)	Serum AST (U/L)	Serum albumin (g/dl)	Serum AFP (IU/L)
Normal-untreated group	18.58 ± 0.18	70.13 ± 0.86	3.92 ± 0.09	0.29 ± 0.02
PVP-AgNPs (30)-control group	18.38 ± 0.19	68.26 ± 0.82	3.94 ± 0.12	0.30 ± 0.01
PVP-AgNPs (125)-control group	18.71 ± 0.19	72.41 ± 0.90	3.88 ± 0.10	0.28 ± 0.01
PVP-AgNPs (300)-control group	21.19 ± 0.15 [a]	81.42 ± 0.84 [a]	3.22 ± 0.11 [a]	0.27 ± 0.01
DEN/CCl4-control group	71.09 ± 0.39 [a]	320.33 ± 2.95 [a]	1.05 ± 0.09 [a]	2.97 ± 0.04 [a]
PVP-AgNPs (30)-treated group	56.66 ± 0.22 [a,b]	233.50 ± 2.65 [a,b]	1.38 ± 0.09 [a]	1.97 ± 0.03 [a,b]
PVP-AgNPs (125)-treated group	28.66 ± 0.32 [a,b,c]	168.92 ± 1.73 [a,b,c]	2.09 ± 0.11 [a,b, c]	0.67 ± 0.02 [a,b,c]
PVP-AgNPs (300)-treated group	30.86 ± 0.55 [a,b,c]	187.29 ± 0.64 [a,b,c,d]	1.92 ± 0.10 [a,b,c,d]	0.86 ± 0.01 [a,b,c,d]

Data were expressed as means ± SEM. [a]$p < 0.05$ compared to the normal-untreated group. [b]$p < 0.05$ compared to DEN/CCl_4–control group. [c]$p < 0.05$ compared to PVP-AgNPs (30)-treated group. [d]$p < 0.05$ compared to PVP-AgNPs (125)-treated group.

Table (2): Effects of PVP-AgNP on DEN/CCl_4-induced HCC regarding the histopathological scoring.

Study Groups (n=12)	Hepatic architecture			N/C ratio					Degree of pleomorphism					Steatosis				
	0	1	Total	0	1	2	3	Total	0	1	2	3	Total	0	1	2	3	Total
Normal-untreated group	12	0	12	12	0	0	0	12	12	0	0	0	12	12	0	0	0	12
PVP-AgNPs (30)-control group	12	0	12	12	0	0	0	12	12	0	0	0	12	12	0	0	0	12
PVP-AgNPs (125)-control group	12	0	12	12	0	0	0	12	12	0	0	0	12	12	0	0	0	12
PVP-AgNPs (300)-control group	11	1	12	12	0	0	0	12	12	0	0	0	12	10	2	0	0	12 [a]
DEN/CCl4-control group	1	6	7 [a]	0	0	1	6	7 [a]	0	0	3	4	7 [a]	0	0	2	5	7 [a]
PVP-AgNPs (30)-treated group	4	2	8 [a,b]	1	1	5	1	8 [a,b]	1	3	4	0	8 [a,b]	4	3	1	0	8 [a,b]
PVP-AgNPs (125)-treated group	10	1	11 [b,c]	9	2	0	0	11 [b,c]	10	1	0	0	11 [a,b,c]	9	1	1	0	11 [a,b,c]
PVP-AgNPs (300)-treated group	8	2	10 [a,b,c,d]	6	3	1	0	10 [a,b,c,d]	7	2	1	0	10 [a,b,c,d]	6	2	2	0	10 [a,b,d]

n=12. Chi-square test with Yates's correction was used to analyzed data. [a]$p < 0.05$ compared to the normal-untreated group. [b]$p < 0.05$ compared to DEN/CCl_4–control group. [c]$p < 0.05$ compared to PVP-AgNPs (30)-treated group. [d]$p < 0.05$ compared to PVP-AgNPs (125)-treated group. N/C ratio: Nuclear/cytoplasmic ratio; DEN: Diethylnitrosamine; CCl4: carbon tetrachloride; PVP-AgNPs: polyvinylpyrrolidone capped-silver nanoparticles.

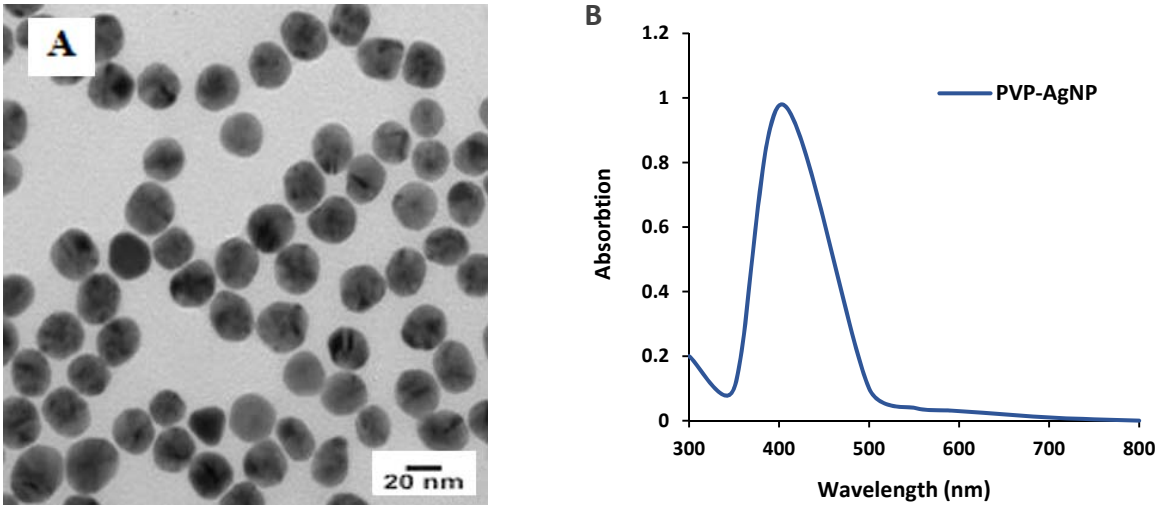

Figure 1: The characterization of PVP-AgNP. (A): TEM photographs of PVP-AgNP with a particle size of 20 nm. (B): The UV-Vis absorption spectrum presented a narrow peak (λ_{max}) at 403 nm, which indicated monodispersed, uniform, and spherical shaped nanoparticles.

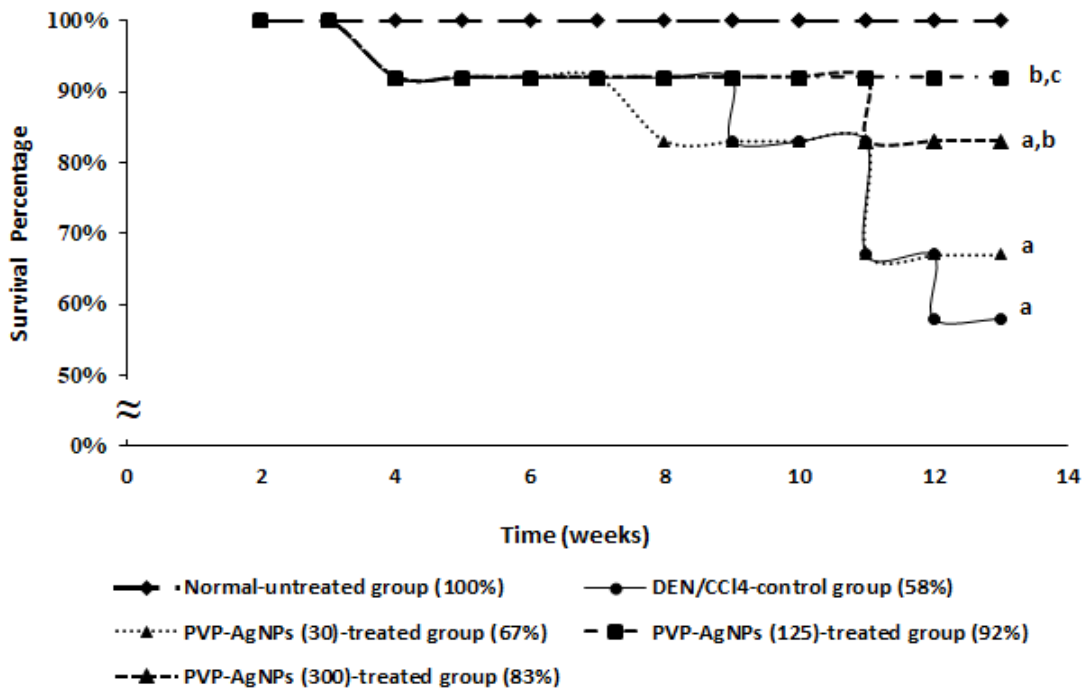

Figure 2: Effects of the **PVP-AgNPs-(30), (125), and (300) on the survival rates**. Values were analyzed by Kaplan–Meier analysis, using Log-Rank test. n= 12. The mean difference was statistically significant at $p < 0.05$. [a]$p < 0.05$ compared to the normal-untreated group. [b]$p < 0.05$ compared to DEN/CCl_4–control group. [c]$p < 0.05$ compared to PVP-AgNPs (30)-treated group. [d]$p < 0.05$ compared to PVP-AgNPs (125)-treated group.

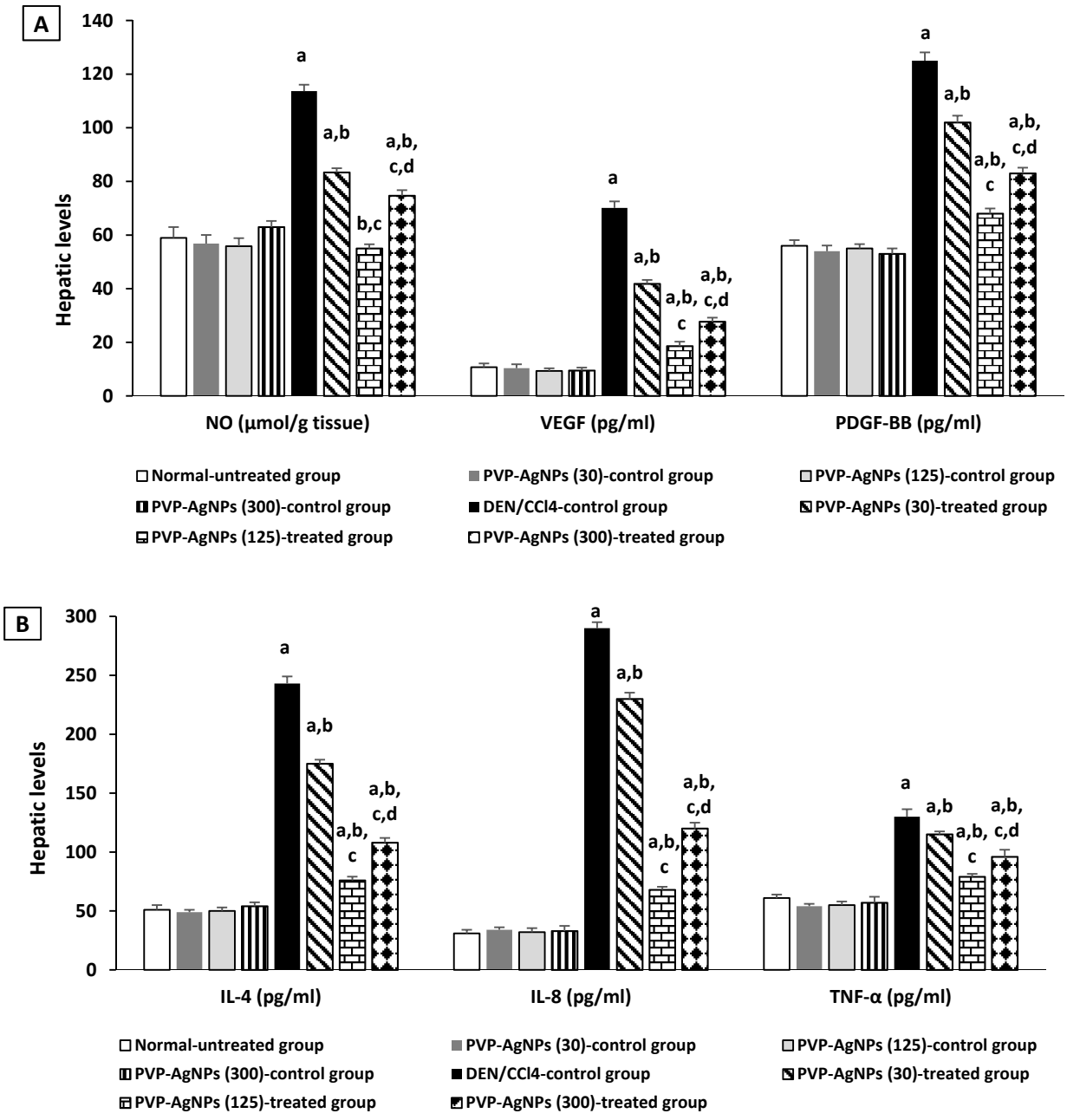

Figure 3: Changes in means hepatic (A) No, Il-4, Il-8, and (B) VEGF, PDGF-BB, and TNF-α levels in different study groups. n=12. [a]$p < 0.05$ compared to the normal-untreated group. [b]$p < 0.05$ compared to PVP-AgNPs (30)-control group. [c]$p < 0.05$ compared to PVP-AgNPs (125)-control group. [d]$p < 0.05$ compared to DEN/CCl_4–control group. [e]$p < 0.05$ compared to PVP-AgNPs (30)-treated group. [f]$p < 0.05$ compared to PVP-AgNPs (125)-treated group.

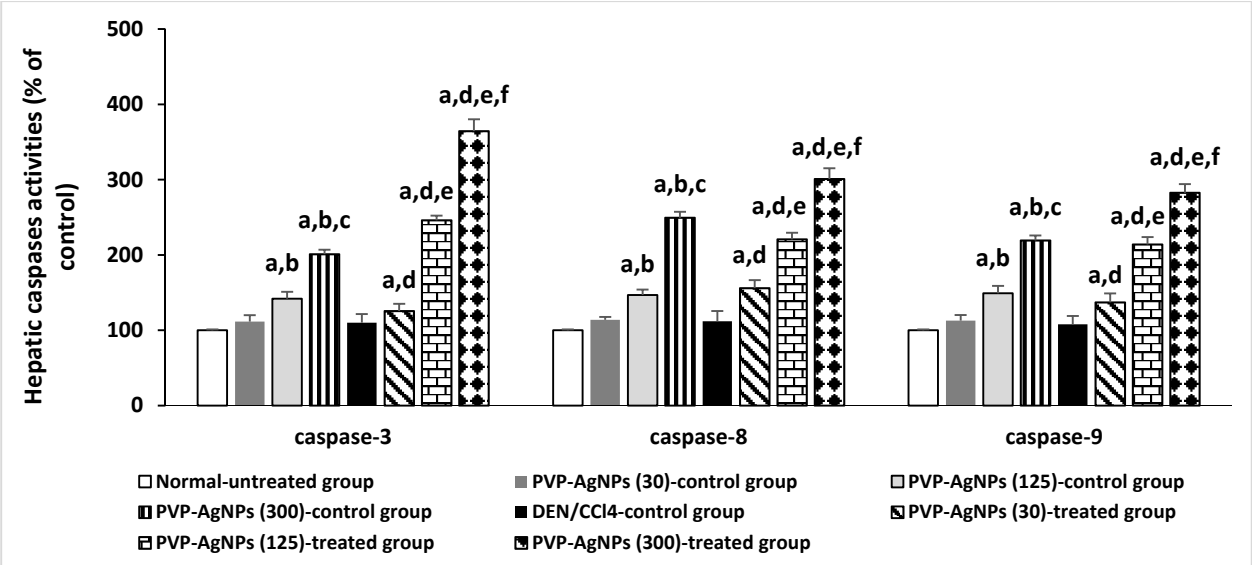

Figure 4: The hepatic activities of caspase-3, -8, and -9 in different study groups. n=12. [a]$p < 0.05$ compared to the normal-untreated group. [b]$p < 0.05$ compared to PVP-AgNPs (30)-control group. [c]$p < 0.05$ compared to PVP-AgNPs (125)-control group. [d]$p < 0.05$ compared to DEN/CCl_4–control group. [e]$p < 0.05$ compared to PVP-AgNPs (30)-treated group. [f]$p < 0.05$ compared to PVP-AgNPs (125)-treated group.

Normal-untreated group

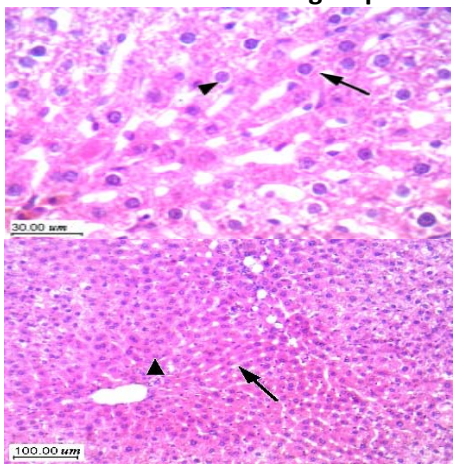

PVP-AgNPs (30)-control group

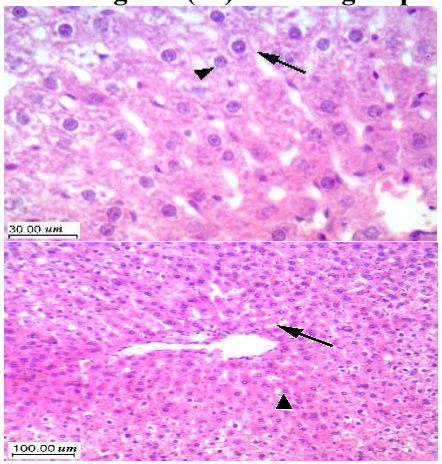

PVP-AgNPs (125)-control group

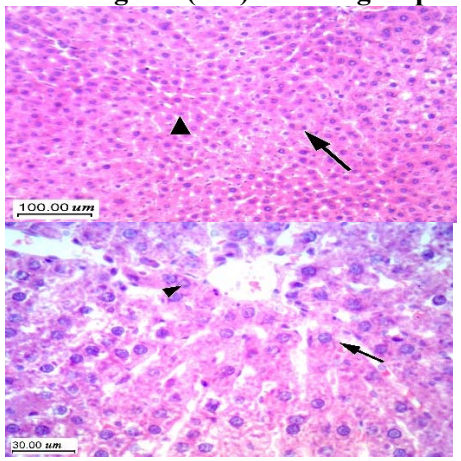

PVP-AgNPs (300)-control group

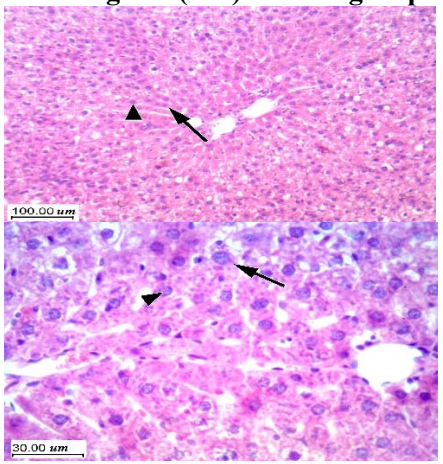

DEN/CCl_4-control group

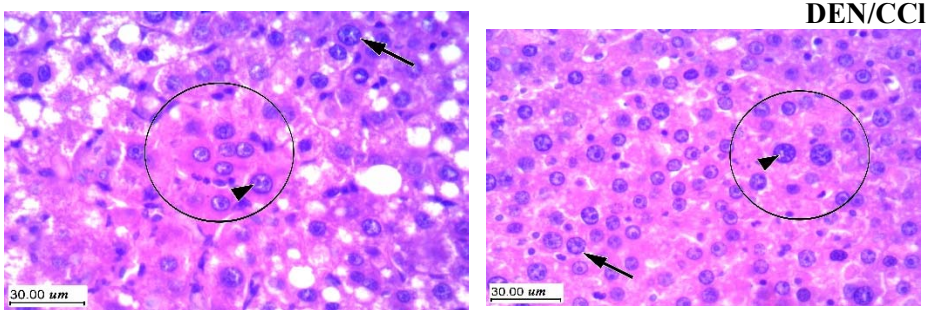

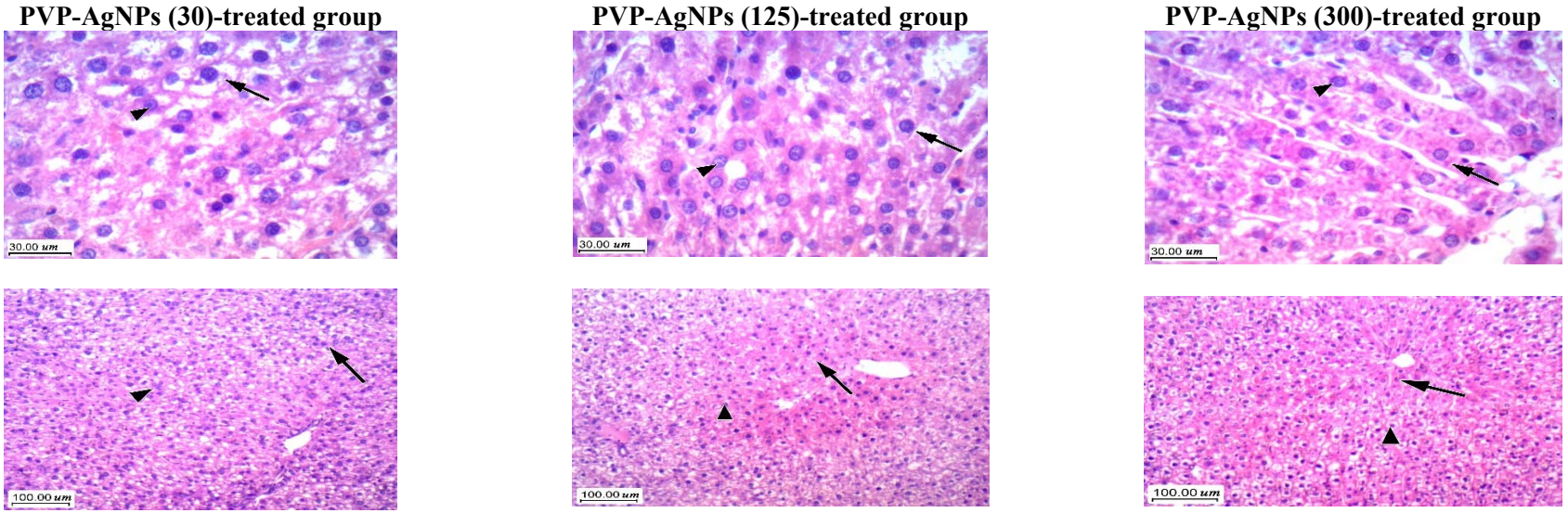

Figure (5): Hepatic histopathological photomicrographs of different study groups stained with hematoxylin & eosin (H&E, 400X and 100X). Normal-untreated group, and the PVP-AgNP (30)-, (125)-, and (300) control groups showed hepatocytes arranged in thin plates with preserved architecture, small nuclei and patent sinusoids. DEN/CCl_4-control group displayed marked disturbed architecture of thick plates, nests and sheets of hepatocytes, which displayed markedly enlarged nuclei, increased nucleo-cytoplasmic ratio (1:1 or more), and nuclei's coarse chromatin, with more than one prominent nucleolus, moderate pleomorphism, and few apoptotic and necrotic cells. The PVP-AgNP (30)-, and (300)-treated groups showed mild, and moderate improvements in the architecture; respectively. The PVP-AgNPs (125)-treated group showed marked improvements with almost restored lobular architecture and hepatocytes with small nuclei and abundant eosinophilic cytoplasm. Arrows: Normal hepatocytes or hepatocytes with increased N/C ratio, Arrow head: Nucleus with inconspicuous nucleoli or prominent nucleoli.

4. DISCUSSION

In the DEN/CCl_4-chemical model of HCC in animals, a multi-step hepatic carcinogenesis is performed, where the DEN-initiation phase is followed by the CCl_4-promotion phase. The DEN is an *N*-nitroso alkylating agent, which is rapidly metabolized and accumulated in the liver, ending in the formation of various DNA adducts as the *O*4-ethyldeoxythymidine, and finally mutations **(Zalatnai and Lapis, 1994; Motawi et al., 2016)**. The promotion with CCl_4 is leading to the hepatic cirrhosis, carcinogenesis, and HCC mimicking the human histopathological and clinical pictures **(Uehara et al., 2013)**.

In the current rat model of HCC-induced by DEN/CCl_4-challenging, the evaluation of the antiangiogenic and apoptotic properties of the PVP-AgNPs were assessed, in addition to serum liver functions, albumin, and AFP levels, as well as how these parameters were affecting the survival rates.

In the present study, the used PVP-AgNPs particles were administered orally. They were in the spherical shape of 20 nm diameter. In general, various capping agents, as PVP which is a safe water-soluble polymer **(Kang et al., 2011; Lima et al., 2012)**, could be added to nanoparticles for thermodynamic stabilization, prevention of the aggregation and enhancing the solubility **(Singh et al., 2009; Seabra and Durán, 2010)**. Additionally, in normal rats, the orally administered 20 nm AgNPs are absorbed extensively in the micelles and are subjected to an extensive hepatic first-pass effect, with a final biliary excretion. The deposition of the un-excreted 20 nm AgNPs was evidenced mainly in the kupffer cells, and sinusoidal endothelium, with an unremarkable deposition in other tissues **(Kim et al., 2010; Jiménez-Lamana et al., 2014)**. Furtherly, the small-sized AgNPs (20 nm) display selective deep tumor cells' permeations in comparison to the larger sized particles (60 and 100 nm) **(AshaRani et al., 2009; Perrault et al., 2009; Prabhu et al., 2011)**.

Presently, the DEN/CCl_4-challenging revealed reductions in the rats' survival rates and serum albumin levels, and increases in serum ALT, AST, and AFP levels. During the previously evidenced DEN/CCl_4-induced carcinogenesis, significant reductions in survival rates, and impairments in liver functions, and serum albumin were reported, which were due to oxidative burden, lipid peroxidation of the hepatocytes' cellular and mitochondrial membranes, and the DNA damage **(Uehara et al., 2013; Ding et al., 2017)**. Moreover, clinically, AFP is considering a non-invasive diagnostic and prognostic factor for HCC, which implicates the HCC incidence, the response to treatment, and the recurrence **(Cheng et al., 2014)**.

Of notice, in Dalton's lymphoma ascites tumor mice model, AgNPs enhanced the survival rates by 50% in comparison to the model controls **(Sriram et al., 2010)**. In the current study, the DEN/CCl_4-induced carcinogenic deleterious effects were ameliorated by the daily oral PVP-AgNPs with higher survival rates. Three different doses of 30, 125, and 300 mg/kg/day were used, from which the dose of 125mg/kg/day exhibited the most therapeutic effects. This could be explained as the therapeutic roles of AgNPs in cancers are evidenced cytotoxic effects which could be obtained starting from the LOAEL (125 or 300 mg/kg/day) in different rat species, and via the oxidative/apoptotic effects on the dysplastic hepatocytes **(Hsin et al., 2008; Sun et al., 2013)**, with remaining of the normal survivors of surrounding hepatocytes.

Upon gut absorption, the AgNPs could behave into two alternative pathways. The first is belonging to the stability of the AgNPs in the Nano-forms, whereas the other pathway is directed into oxidative dissolution with Ag release (Loeschner et al., 2011; Vandebriel et al., 2014). The earlier study demonstrated that the accumulation and penetration of AgNps into the hepatic pool is a concentration-dependent regardless the administration duration. With higher AgNPs concentrations, the hepatocellular mitochondrial saturation occurs, leading to marked AgNPs accumulation in the residual cellular parts. Moreover, Ag oxides, which form insides the cells, has the ability to initiate complexes with the abundant proteins in the cellular environment, especially the cysteine-rich residues. These proteins have a major role in the activation/suppression of various growth factors and their receptors at the cellular levels (Coyle et al., 2002; Jiménez-Lamana et al., 2014).

In the current study, the DEN/CCl4-challenging revealed increases in the hepatic angiogenic factors; NO, Il-4, Il-8, VEGF, and PDGF. In HCC, poor prognosis is associated with upregulated angiogenic factors and excessive tumor vasculature. In dynamic paracrine and autocrine manners, the hepatic stromal, tumor and stellate cells are considering major sources of these angiogenic factors **(Zhu et al., 2011, 2015; Muto et al., 2015; Otto et al., 2017)**.

The higher hepatic NO production is playing very important roles in neoplastic transformation and progression through DNA damage. Moreover, the hepatic cancer cells with multidrug resistance protein-1 (MDR1) phenotype display marked inducible nitric oxide synthase expression and NO levels **(Fantappiè et al., 2015; de Oliveira et al., 2017)**. Of the most important regulating, prognostic, and aggressive angiogenic factors are VEGF, and PDGF which are promising therapeutic targets in HCC. In HCC, VEGF, via its receptors, is correlated with higher dysplastic grades, and vascular invasion **(Sanz-Cameno et al.,**

2010; Coulouarn and Clément, 2014; Zhu et al., 2015). Whereas, PDGF is stabilizing the new vascular architecture through regulation of the endothelial tubular investment with pericytes and mural cells **(Zhu et al., 2011; Muto et al., 2015; Talaat et al., 2016)**.

In the present work, PVP-AgNPs administration displayed significant reductions in the DEN/CCl_4-induced angiogenesis. Preceding results on the cellular effects of AgNPs showed disruption in the Hypoxia-inducible factor-1/VEGF signaling pathway by which the inhibition of angiogenesis and cancer cell growth were obtained **(Yang et al., 2016)**. In accordance, in bovine retinal endothelial cells, AgNPs reduced the VEGF-induced cellular proliferation and migration through enhanced caspase-3 activity and reduction in PI3K/AKT dependent pathway **(Kalishwaralal et al., 2009)**. In contrast to the present results, Kang and colleagues (2011) reported that PVP-AgNPs particles in a diameter of 2.3 nm induced endothelial cell tube formation with upregulation of VEGF, and NO in a *vitro* endothelial cell line, SVEC4-10. The differences of AgNPs particles diameter with extensive permeation and the lake of paracrine signals for HCC could explain this discrepancy.

Regarding IL-4, higher levels are evidenced by the different stages of HCC. Of note, IL-4 is enhancing the angiogenesis, and the tumor growth and metastasis and are suppressing the cytotoxic T-lymphocytes-derived apoptosis and the M2 macrophages polarization with the formation of tumor-associated macrophages **(Fan et al., 2014; Gao et al., 2015; Ouyang et al., 2016; Akkari and Lujambio, 2017; Guo et al., 2017)**. In addition, IL-8, an effective pro-inflammatory cytokine, could enhance the VEGF expression through the expressional upregulation of hypoxia-inducible factor-1, nuclear factor-κB, and Signal Transducer and Activator of Transcription-3 transcriptional factors **(Martin et al., 2009; Chen et al., 2014; Zhu et al., 2015)**.

In the present work, significant reductions in hepatic IL-4, and IL-8 were evident after different therapeutic regimens of PVP-AgNPs. **Park et al. (2010)** concluded that AgNps in a size of 42nm could elevate serum IL-4 with the repeated administration for 28 days.

As an inflammatory, apoptotic, and angiogenic cytokine, TNF-α has various important roles in HCC pathogenesis. It leads to superoxide formation, with either activation of the caspase-8, and/or induction of necroptosis. The necroptosis cell death is a consequence of caspase inactivity with the engagement of death receptors mainly TNF receptor-1 (TNFR1). Moreover, the upregulated expression of VEGF/VEGF receptors and IL-8 are evidenced after TNF-α production **(Park et al., 2010; Zhu et al., 2011; Shalini et al., 2015; Talaat et al., 2016)**. Presently, PVP-AgNPs regimens decreased the hepatic TNF-α levels, which could explain the reduction in the hepatic VEGF, and IL-8 levels, and activation of hepatic caspase-8.

In HCC, the growth and proliferation of dysplastic hepatocytes, and activated Kupffer cells, and the oxidative/inflammatory/angiogenic signaling pathways are facilitating the primary tumor dissemination and are protecting its survival with dysregulation of the apoptosis **(Fabregat, 2009)**. The dysregulated apoptosis expanses the cancer cells mass with consequent therapeutic resistance **(Im et al., 2017)**. In the current work, DEN/CCl_4-challenging revealed insignificant elevations in hepatic caspases activity. The caspases-dependent apoptosis is an important therapeutic pathway in cancer. The caspase-3 is an executioner one, which activated through various signaling pathways by caspase-8 or caspase-9 **(Chang et al., 2015; Shalini et al., 2015; Ding et al., 2017)**.

Through its cytotoxic effects, AgNPs could enhance the proteolytic activities of different caspases **(Kalishwaralal et al., 2009; Gaiser et al., 2013)**. These findings are in agreement with our outcomes, where PVP-AgNPs augments the hepatic caspases-3, -8, -9 activities. Earlier, PVP-AgNPs administration revealed that the apoptosis cascades of PVP-AgNPs could be through the generation of reactive oxygen specious and c-Jun N-terminal kinases (JNK) **(Hsin et al., 2008)**.

Of notice, the dampening of inflammation is evident in the apoptotic course through inactivation of different inflammatory pathways **(Martin et al., 2012; Creagh, 2014)**. This furtherly mitigates the TNFR1 and other death receptors stimulations result in further caspases activations **(Creagh, 2014)**. These finding could explain how AgNPs could modulate the inflammatory/apoptotic pathways in HCC milieu.

In accordance with previous histopathological findings **(Abdel aziz et al., 2011; Motawi et al., 2016; Ding et al., 2017)**, the challenging with DEN/CCl_4 revealed marked distortion in the hepatic architecture and higher dysplastic changes. In obvious manners, significant ameliorations in these dysplastic changes and restoration of hepatic architectures were evident after the therapeutic regimens of PVP-AgNPs, mainly in the dose of 125 mg/kg/day. These outcomes were consistent with the above current results of PVP-AgNPs regarding the serum liver enzymes, albumin, and AFP levels, and the inflammatory, apoptotic, and angiogenic parameters.

5. CONCLUSION

In conclusion, PVP-AgNPs in a dose of 125mg/kg/day could be considered a cytotoxic therapy for HCC with anti-inflammatory, anti-angiogenic, and apoptotic proprieties, in addition to the improvement in survival rates. Further studies are in need for targeting other molecular signaling pathways related to PVP-AgNPs therapeutic approaches in HCC. Moreover, additional chronological studies should be done for assessment of the therapeutic effects of PVP-AgNPs

alone and in combination with other chemotherapeutic regimens used for HCC treatment.

Conflict of interest

The authors declare that they have no conflict of interest.

6. REFERENCES

Abdel aziz, M.T., El Asmar, M.F., Atta, H.M., Mahfouz, S., Fouad, H.H., Roshdy, N.K., Rashed, L.A., Sabry, D., Hassouna, A.A., Taha, F.M., 2011. Efficacy of mesenchymal stem cells in suppression of hepatocarcinorigenesis in rats: possible role of Wnt signaling. J. Exp. Clin. Cancer Res. CR 30, 49. https://doi.org/10.1186/1756-9966-30-49

Akkari, L., Lujambio, A., 2017. Role of Tumor Microenvironment in Hepatocellular Carcinoma Resistance, in: Resistance to Molecular Therapies for Hepatocellular Carcinoma, Resistance to Targeted Anti-Cancer Therapeutics. Springer, Cham, pp. 45–64. https://doi.org/10.1007/978-3-319-56197-4_3

AshaRani, P., Hande, M.P., Valiyaveettil, S., 2009. Anti-proliferative activity of silver nanoparticles. BMC Cell Biol. 10, 65. https://doi.org/10.1186/1471-2121-10-65

Billmire, D.F., Cullen, J.W., Rescorla, F.J., Davis, M., Schlatter, M.G., Olson, T.A., Malogolowkin, M.H., Pashankar, F., Villaluna, D., Krailo, M., Egler, R.A., Rodriguez-Galindo, C., Frazier, A.L., 2014. Surveillance after initial surgery for pediatric and adolescent girls with stage I ovarian germ cell tumors: report from the Children's Oncology Group. J. Clin. Oncol. Off. J. Am. Soc. Clin. Oncol. 32, 465–470. https://doi.org/10.1200/JCO.2013.51.1006

Bishayee, A., S. Darvesh, A., 2012. Angiogenesis in Hepatocellular Carcinoma: A Potential Target for Chemoprevention and Therapy. Curr. Cancer Drug Targets 12, 1095–1118.

Chang, J.-S., Kuo, H.-P., Chang, K.L.B., Kong, Z.-L., 2015. Apoptosis of Hepatocellular Carcinoma Cells Induced by Nanoencapsulated Polysaccharides Extracted from Antrodia Camphorata. PLOS ONE 10, e0136782. https://doi.org/10.1371/journal.pone.0136782.

Chen, L., Fan, J., Chen, H., Meng, Z., Chen, Z., Wang, P., Liu, L., 2014. The IL-8/CXCR1 axis is associated with cancer stem cell-like properties and correlates with clinical prognosis in human pancreatic cancer cases. Sci. Rep. 4, 5911. https://doi.org/10.1038/srep05911

Chen, S.-W., Chen, Y.-X., Zhang, X.-R., Qian, H., Chen, W.-Z., Xie, W.-F., 2008. Targeted inhibition of platelet-derived growth factor receptor-beta subunit in hepatic stellate cells ameliorates hepatic fibrosis in rats. Gene Ther. 15, 1424–1435. https://doi.org/10.1038/gt. 2008. 93.

Cheng, J., Wang, W., Zhang, Y., Liu, X., Li, M., Wu, Z., Liu, Z., Lv, Y., Wang, B., 2014. Prognostic Role of Pre-Treatment Serum AFP-L3% in Hepatocellular Carcinoma: Systematic Review and Meta-Analysis. PLoS ONE 9, e87011. https://doi.org/10.1371/journal.pone.0087011

çIftçI, H., TüRk, M., Tamer, U., Karahan, S., Menemen, Y., 2013. Silver nanoparticles: cytotoxic, apoptotic, and necrotic effects on MCF-7 cells. Turk. J. Biol. 37, 573–581. https://doi.org/10.3906/biy-1302-21

Coulouarn, C., Clément, B., 2014. Stellate cells and the development of liver cancer: therapeutic potential of targeting the stroma. J. Hepatol. 60, 1306–1309. https://doi.org/10.1016/j.jhep.2014.02.003

Coyle, P., Philcox, J.C., Carey, L.C., Rofe, A.M., 2002. Metallothionein: the multipurpose protein. Cell. Mol. Life Sci. CMLS 59, 627–647. https://doi.org/10.1007/s00018-002-8454-2

Creagh, E.M., 2014. Caspase crosstalk: integration of apoptotic and innate immune signalling pathways. Trends Immunol. 35, 631–640. https://doi.org/10.1016/j.it.2014.10.004

de Lima, R., Seabra, A.B., Durán, N., 2012. Silver nanoparticles: a brief review of cytotoxicity and genotoxicity of chemically and biogenically synthesized nanoparticles. J. Appl. Toxicol. JAT 32, 867–879. https://doi.org/10.1002/jat.2780.

de Oliveira, G.A., Cheng, R.Y.S., Ridnour, L.A., Basudhar, D., Somasundaram, V., McVicar, D.W., Monteiro, H.P., Wink, D.A., 2017. Inducible Nitric Oxide Synthase in the Carcinogenesis of Gastrointestinal Cancers. Antioxid. Redox Signal. 26, 1059–1077. https://doi.org/10.1089/ars.2016.6850.

Ding, Y., Wu, Z., Wei, Y., Shu, L., Peng, Y., 2017. Hepatic inflammation-fibrosis-cancer axis in the rat hepatocellular carcinoma induced by diethylnitrosamine. J. Cancer Res. Clin. Oncol. 143, 821–834. https://doi.org/10.1007/s00432-017-2364-z

Fabregat, I., 2009. Dysregulation of apoptosis in hepatocellular carcinoma cells. World J. Gastroenterol. 15, 513. https://doi.org/10.3748/wjg.15.513.

Fan, Q.-M., Jing, Y.-Y., Yu, G.-F., Kou, X.-R., Ye, F., Gao, L., Li, R., Zhao, Q.-D., Yang, Y., Lu, Z.-H., Wei, L.-X., 2014. Tumor-associated macrophages promote cancer stem cell-like properties via transforming growth factor-beta1-induced epithelial–

mesenchymal transition in hepatocellular carcinoma. Cancer Lett. 352, 160–168. https://doi.org/10.1016/j.canlet.2014.05.008

Fantappiè, O., Sassoli, C., Tani, A., Nosi, D., Marchetti, S., Formigli, L., Mazzanti, R., 2015. Mitochondria of a human multidrug-resistant hepatocellular carcinoma cell line constitutively express inducible nitric oxide synthase in the inner membrane. J. Cell. Mol. Med. 19, 1410–1417. https://doi.org/10.1111/jcmm.12528

Fornari, F., Pollutri, D., Patrizi, C., Bella, T.L., Marinelli, S., Gardini, A.C., Marisi, G., Toaldo, M.B., Baglioni, M., Salvatore, V., Callegari, E., Baldassarre, M., Galassi, M., Giovannini, C., Cescon, M., Ravaioli, M., Negrini, M., Bolondi, L., Gramantieri, L., 2017. In hepatocellular carcinoma miR-221 modulates Sorafenib resistance through inhibition of caspase-3 mediated apoptosis. Clin. Cancer Res. clincanres.1464.2016. https://doi.org/10.1158/1078-0432.CCR-16-1464

Gaiser, B.K., Hirn, S., Kermanizadeh, A., Kanase, N., Fytianos, K., Wenk, A., Haberl, N., Brunelli, A., Kreyling, W.G., Stone, V., 2013. Effects of Silver Nanoparticles on the Liver and Hepatocytes In Vitro. Toxicol. Sci. 131, 537–547. https://doi.org/10.1093/toxsci/kfs306

Gao, S., Zhou, J., Liu, N., Wang, L., Gao, Q., Wu, Y., Zhao, Q., Liu, P., Wang, S., Liu, Y., Guo, N., Shen, Y., Wu, Y., Yuan, Z., 2015. Curcumin induces M2 macrophage polarization by secretion IL-4 and/or IL-13. J. Mol. Cell. Cardiol. 85, 131–139. https://doi.org/10.1016/j.yjmcc.2015.04.025

Guo, C., Ouyang, Y., Cai, J., Xiong, L., Chen, Y., Zeng, X., Liu, A., 2017. High expression of IL-4R enhances proliferation and invasion of hepatocellular carcinoma cells. Int. J. Biol. Markers 32, e384–e390. https://doi.org/10.5301/ijbm.5000280.

Gurunathan, S., Lee, K.-J., Kalishwaralal, K., Sheikpranbabu, S., Vaidyanathan, R., Eom, S.H., 2009. Antiangiogenic properties of silver nanoparticles. Biomaterials 30, 6341–6350. https://doi.org/10.1016/j.biomaterials.2009.08.008

Hsin, Y.-H., Chen, C.-F., Huang, S., Shih, T.-S., Lai, P.-S., Chueh, P.J., 2008. The apoptotic effect of nanosilver is mediated by a ROS- and JNK-dependent mechanism involving the mitochondrial pathway in NIH3T3 cells. Toxicol. Lett. 179, 130–139. https://doi.org/10.1016/j.toxlet.2008.04.015

Huo, H.Z., Wang, B., Liang, Y.K., Bao, Y.Y., Gu, Y., 2011. Hepatoprotective and Antioxidant Effects of Licorice Extract against CCl4-Induced Oxidative Damage in Rats. Int. J. Mol. Sci. 12, 6529–6543. https://doi.org/10.3390/ijms12106529

Hussein, R., Sarhan, O., 2014. Effects of intraperitoneally injected silver nanoparticles on histological structures and blood parameters in the albino rat. Int. J. Nanomedicine 1505. https://doi.org/10.2147/IJN.S56729

Im, E., Yeo, C., Lee, H.-J., Lee, E.-O., 2017. Dihydroartemisinin induced caspase-dependent apoptosis through inhibiting the specificity protein 1 pathway in hepatocellular carcinoma SK-Hep-1 cells. Life Sci. https://doi.org/10.1016/j.lfs.2017.11.008

Jiménez-Lamana, J., Laborda, F., Bolea, E., Abad-Álvaro, I., Castillo, J.R., Bianga, J., He, M., Bierla, K., Mounicou, S., Ouerdane, L., Gaillet, S., Rouanet, J.-M., Szpunar, J., 2014. An insight into silver nanoparticles bioavailability in rats. Met. Integr. Biometal Sci. 6, 2242–2249. https://doi.org/10.1039/c4mt00200h

Kalishwaralal, K., Banumathi, E., Pandian, S.R.K., Deepak, V., Muniyandi, J., Eom, S.H., Gurunathan, S., 2009. Silver nanoparticles inhibit VEGF induced cell proliferation and migration in bovine retinal endothelial cells. Colloids Surf. B Biointerfaces 73, 51–57. https://doi.org/10.1016/j.colsurfb.2009.04.025

Kang, K., Lim, D.-H., Choi, I.-H., Kang, T., Lee, K., Moon, E.-Y., Yang, Y., Lee, M.-S., Lim, J.-S., 2011. Vascular tube formation and angiogenesis induced by polyvinylpyrrolidone-coated silver nanoparticles. Toxicol. Lett. 205, 227–234. https://doi.org/10.1016/j.toxlet.2011.05.1033

Kim, Y.S., Song, M.Y., Park, J.D., Song, K.S., Ryu, H.R., Chung, Y.H., Chang, H.K., Lee, J.H., Oh, K.H., Kelman, B.J., Hwang, I.K., Yu, I.J., 2010. Subchronic oral toxicity of silver nanoparticles. Part. Fibre Toxicol. 7, 20. https://doi.org/10.1186/1743-8977-7-20

Kleiner, D.E., Brunt, E.M., Van Natta, M., Behling, C., Contos, M.J., Cummings, O.W., Ferrell, L.D., Liu, Y.-C., Torbenson, M.S., Unalp-Arida, A., Yeh, M., McCullough, A.J., Sanyal, A.J., Nonalcoholic Steatohepatitis Clinical Research Network, 2005. Design and validation of a histological scoring system for nonalcoholic fatty liver disease. Hepatol. Baltim. Md 41, 1313–1321. https://doi.org/10.1002/hep.20701

Lee, P.C., Meisel, D., 1982. Adsorption and surface-enhanced Raman of dyes on silver and gold sols. J. Phys. Chem. 86, 3391–3395. https://doi.org/10.1021/j100214a025

Loeschner, K., Hadrup, N., Qvortrup, K., Larsen, A., Gao, X., Vogel, U., Mortensen, A., Lam, H.R., Larsen, E.H., 2011. Distribution of silver in rats following 28 days of repeated oral exposure to silver

nanoparticles or silver acetate. Part. Fibre Toxicol. 8, 18. https://doi.org/10.1186/1743-8977-8-18

Martin, D., Galisteo, R., Gutkind, J.S., 2009. CXCL8/IL8 Stimulates Vascular Endothelial Growth Factor (VEGF) Expression and the Autocrine Activation of VEGFR2 in Endothelial Cells by Activating NFκB through the CBM (Carma3/Bcl10/Malt1) Complex. J. Biol. Chem. 284, 6038–6042. https://doi.org/10.1074/jbc.C800207200

Martin, S.J., Henry, C.M., Cullen, S.P., 2012. A perspective on mammalian caspases as positive and negative regulators of inflammation. Mol. Cell 46, 387–397. https://doi.org/10.1016/j.molcel.2012.04.026

Montgomery, H. a. C., Dymock, J.F., Thom, N.S., 1962. The rapid colorimetric determination of organic acids and their salts in sewage-sludge liquor. Analyst 87, 949–955. https://doi.org/10.1039/AN9628700949

Motawi, T.K., El-Boghdady, N.A., El-Sayed, A.M., Helmy, H.S., 2016. Comparative study of the effects of PEGylated interferon-α2a versus 5-fluorouracil on cancer stem cells in a rat model of hepatocellular carcinoma. Tumor Biol. 37, 1617–1625. https://doi.org/10.1007/s13277-015-3920-2

Muto, J., Shirabe, K., Sugimachi, K., Maehara, Y., 2015. Review of angiogenesis in hepatocellular carcinoma: Angiogenesis in hepatocellular carcinoma. Hepatol. Res. 45, 1–9. https://doi.org/10.1111/hepr.12310

Njei, B., Rotman, Y., Ditah, I., Lim, J.K., 2015. Emerging trends in hepatocellular carcinoma incidence and mortality. Hepatol. Baltim. Md 61, 191–199. https://doi.org/10.1002/hep.27388

Otto, W., Sierdziński, J., Król, M., Wolińska, E., Feliksbrot-Bratosiewicz, M., Wilkowojska, U., 2017. The value of tumor angiogenesis activity for stratification of HCC patients. Int. J. Clin. Exp. Med. 10, 4200–4213.

Ouyang, F.-Z., Wu, R.-Q., Wei, Y., Liu, R.-X., Yang, D., Xiao, X., Zheng, L., Li, B., Lao, X.-M., Kuang, D.-M., 2016. Dendritic cell-elicited B-cell activation fosters immune privilege via IL-10 signals in hepatocellular carcinoma. Nat. Commun. 7. https://doi.org/10.1038/ncomms13453

Pacioni, N.L., Borsarelli, C.D., Rey, V., Veglia, A.V., 2015. Synthetic Routes for the Preparation of Silver Nanoparticles, in: Alarcon, E.I., Griffith, M., Udekwu, K.I. (Eds.), Silver Nanoparticle Applications. Springer International Publishing, Cham, pp. 13–46. https://doi.org/10.1007/978-3-319-11262-6_2

Paradis, V., 2013. Histopathology of hepatocellular carcinoma. Recent Results Cancer Res. Fortschritte Krebsforsch. Progres Dans Rech. Sur Cancer 190, 21–32. https://doi.org/10.1007/978-3-642-16037-0_2

Park, E.-J., Bae, E., Yi, J., Kim, Y., Choi, K., Lee, S.H., Yoon, J., Lee, B.C., Park, K., 2010. Repeated-dose toxicity and inflammatory responses in mice by oral administration of silver nanoparticles. Environ. Toxicol. Pharmacol. 30, 162–168. https://doi.org/10.1016/j.etap.2010.05.004

Park, E.J., Lee, J.H., Yu, G.-Y., He, G., Ali, S.R., Holzer, R.G., Osterreicher, C.H., Takahashi, H., Karin, M., 2010. Dietary and genetic obesity promote liver inflammation and tumorigenesis by enhancing IL-6 and TNF expression. Cell 140, 197–208. https://doi.org/10.1016/j.cell.2009.12.052

Perrault, S.D., Walkey, C., Jennings, T., Fischer, H.C., Chan, W.C.W., 2009. Mediating tumor targeting efficiency of nanoparticles through design. Nano Lett. 9, 1909–1915. https://doi.org/10.1021/nl900031y

Prabhu, V., Uzzaman, S., Grace, V.M.B., Guruvayoorappan, C., 2011. Nanoparticles in Drug Delivery and Cancer Therapy: The Giant Rats Tail. J. Cancer Ther. 2. https://doi.org/10.4236/jct.2011.23045

Sanz-Cameno, P., Trapero-Marugán, M., Chaparro, M., Jones, E.A., Moreno-Otero, R., 2010. Angiogenesis: From Chronic Liver Inflammation to Hepatocellular Carcinoma. J. Oncol. 2010, 1–7. https://doi.org/10.1155/2010/272170

Seabra, A.B., Durán, N., 2010. Nitric oxide-releasing vehicles for biomedical applications. J Mater Chem 20, 1624–1637. https://doi.org/10.1039/B912493B

Shalini, S., Dorstyn, L., Dawar, S., Kumar, S., 2015. Old, new and emerging functions of caspases. Cell Death Differ. 22, 526–539. https://doi.org/10.1038/cdd.2014.216

Singh, S., Patel, P., Jaiswal, S., Prabhune, A.A., Ramana, C.V., Prasad, B.L.V., 2009. A direct method for the preparation of glycolipid–metal nanoparticle conjugates: sophorolipids as reducing and capping agents for the synthesis of water re-dispersible silver nanoparticles and their antibacterial activity. New J Chem 33, 646–652. https://doi.org/10.1039/B811829A

Sriram, M.I., Kanth, S.B.M., Kalishwaralal, K., Gurunathan, S., 2010. Antitumor activity of silver nanoparticles in Dalton's lymphoma ascites tumor model. Int. J. Nanomedicine 5, 753–762. https://doi.org/10.2147/IJN.S11727

Sun, X., Wang, Z., Zhai, S., Cheng, Y., Liu, J., Liu, B., 2013. In vitro cytotoxicity of silver nanoparticles in primary rat hepatic stellate cells. Mol. Med. Rep. 8, 1365–1372. https://doi.org/10.3892/mmr.2013.1683

Talaat, R.M., Adel, S., Salem, T.A., Nasr, M.I., 2016. Correlation between angiogenic/inflammatory mediators in Wister rat model of liver dysplasia. J. Immunoassay Immunochem. 37, 472–484. https://doi.org/10.1080/15321819.2016.1157490

Uehara, T., Ainslie, G.R., Kutanzi, K., Pogribny, I.P., Muskhelishvili, L., Izawa, T., Yamate, J., Kosyk, O., Shymonyak, S., Bradford, B.U., Boorman, G.A., Bataller, R., Rusyn, I., 2013. Molecular Mechanisms of Fibrosis-Associated Promotion of Liver Carcinogenesis. Toxicol. Sci. 132, 53–63. https://doi.org/10.1093/toxsci/kfs342

Vandebriel, R.J., Tonk, E.C., de la Fonteyne-Blankestijn, L.J., Gremmer, E.R., Verharen, H.W., van der Ven, L.T., van Loveren, H., de Jong, W.H., 2014. Immunotoxicity of silver nanoparticles in an intravenous 28-day repeated-dose toxicity study in rats. Part. Fibre Toxicol. 11, 21. https://doi.org/10.1186/1743-8977-11-21

Wong, R.S., 2011. Apoptosis in cancer: from pathogenesis to treatment. J. Exp. Clin. Cancer Res. CR 30, 87. https://doi.org/10.1186/1756-9966-30-87.

Yang, J., Wang, Q., Qiao, C., Lin, Z., Li, X., Huang, Y., Zhou, T., Li, Y., Shen, B., Lv, M., Feng, J., 2014. Potent anti-angiogenesis and anti-tumor activity of a novel human anti-VEGF antibody, MIL60. Cell. Mol. Immunol. 11, 285–293. https://doi.org/10.1038/cmi.2014.6

Yang, T., Yao, Q., Cao, F., Liu, Q., Liu, B., Wang, X.-H., 2016. Silver nanoparticles inhibit the function of hypoxia-inducible factor-1 and target genes: insight into the cytotoxicity and antiangiogenesis. Int. J. Nanomedicine 11, 6679–6692. https://doi.org/10.2147/IJN.S109695

Yin, W., Nie, Y., Zhang, Z., Xie, L., He, X., 2015. miR-193b acts as a cisplatin sensitizer via the caspase-3-dependent pathway in HCC chemotherapy. Oncol. Rep. https://doi.org/10.3892/or.2015.3996

Yu, S.J., 2016. A concise review of updated guidelines regarding the management of hepatocellular carcinoma around the world: 2010-2016. Clin. Mol. Hepatol. 22, 7–17. https://doi.org/10.3350/cmh.2016.22.1.7

Zalatnai, A., Lapis, K., 1994. Simultaneous induction of liver cirrhosis and hepatocellular carcinomas in F-344 rats: establishment of a short hepatocarcinogenesis model. Exp. Toxicol. Pathol. 46, 215–222. https://doi.org/10.1016/S0940-2993(11)80085-0

Zhu, A.X., Duda, D.G., Sahani, D.V., Jain, R.K., 2011. HCC and angiogenesis: possible targets and future directions. Nat. Rev. Clin. Oncol. 8, 292–301. https://doi.org/10.1038/nrclinonc.2011.30

Zhu, B., Lin, N., Zhang, M., Zhu, Y., Cheng, H., Chen, S., Ling, Y., Pan, W., Xu, R., 2015. Activated hepatic stellate cells promote angiogenesis via interleukin-8 in hepatocellular carcinoma. J. Transl. Med. 13. https://doi.org/10.1186/s12967-015-0730-7